



# A microscopic study on ternary blended cement based composites



Yun Gao<sup>a,\*</sup>, Geert De Schutter<sup>a</sup>, Guang Ye<sup>a,b</sup>, Zhuqing Yu<sup>b</sup>, Zhijun Tan<sup>a</sup>, Kai Wu<sup>a</sup>

<sup>a</sup> Magnel Laboratory for Concrete Research, Department of Structural Engineering, Ghent University, Technologiepark-Zwijnaarde 904, B-9052 Ghent, Belgium

<sup>b</sup> Microlab, Faculty of Civil Engineering and Geosciences, Delft University of Technology, 2628 CN Delft, The Netherlands

## HIGHLIGHTS

- A microscopic investigation is conducted on ternary cementitious composites.
- The phase composition profiles and the degree of hydration are quantified.
- Effects of SCMs, curing age and water binder ratio are discussed.

## ARTICLE INFO

### Article history:

Received 1 March 2013

Received in revised form 5 April 2013

Accepted 9 April 2013

Available online 13 May 2013

### Keywords:

Ternary blended

Replacement levels of SCMs

Curing age

Water binder ratio

ITZ

## ABSTRACT

In this paper, an experimental and numerical study is carried out to investigate the microscopic features of ternary blended cement based composites consisting of ordinary Portland cement, blast furnace slag and limestone filler. In particular, the backscattered electron (BSE) image analysis is utilized to process the experimental measurement, while the continuum type model HYMOSTRUC is employed to conduct the numerical simulation. The effects of various factors including replacement levels of supplementary cementitious materials (SCMs), curing age and water binder (*w/b*) ratio are quantitatively discussed in terms of the phase compositions and the hydration degrees of cementitious materials. Specifically, the area fractions of anhydrous grains and capillary pores are collected with respect to the interfacial transition zone (ITZ) and bulk paste. Results indicate that in the presence of varying SCMs content, curing age and *w/b* ratio, the extent of ITZ almost does not get influenced, whereas the phase compositions are significantly affected.

Crown Copyright © 2013 Published by Elsevier Ltd. All rights reserved.

## 1. Introduction

In recent decades, some new types of concrete, such as high performance concrete (HPC) and self-compacting concrete (SCC) have been developed and applied in industrial practices [1–4]. Compared to conventional concrete, HPC and SCC gain considerable improvements in specific material properties. A key feature of these new materials is the use of supplementary cementitious materials (SCMs). By means of replacing cement with various SCMs, the physical and chemical properties of concrete can be altered. For instance, concrete can obtain a higher strength with the incorporation of silica fume, while fly ash or blast furnace slag blended concrete is often found to be more durable when subjected to aggressive environments [5–7]. To understand how SCMs affect material properties, it is essential to understand how SCMs affect the relevant material structure of concrete.

Concrete is a kind of intrinsic multiscale heterogeneous medium. At the microscopic scale, anhydrous grains and hydration products stack randomly, whereas the solid phases are not able

to fully fill the space, which leads to the formation of a porous structure [8,9]. Furthermore, the formed porous structure spatially varies within concrete. In the presence of aggregate, the normal packing of cementitious particles can be disturbed. In particular, due to the wall effect, large cementitious particles are depleted in the vicinity of aggregates. Afterwards, an excess of porosity can be detected within this specific area, i.e., the interfacial transition zone (ITZ) [10–14]. The ITZ is usually considered to bring a negative impact on overall properties of concrete, such as facilitating the ingress of chemical ions [15,16]. In this regard, the characterization of concrete material structure can be addressed in terms of capturing the microscopic features of ITZ and bulk paste.

For blended cementitious systems, two types of chemical reactions are often referred to during the hardening process, i.e., the hydration of cement and the pozzolanic reaction of SCMs. For instance, within the blast furnace slag blended cement system, the hydration of cement produces calcium hydroxide (CH) which then takes part in the pozzolanic reaction of blast furnace slag [17–20]. The interaction between cement and SCMs makes the relevant microscopic features more complex, where the effects of various hydration factors might be nontrivial [21]. In other words, in the presence of SCMs, the effects of hydration factors, such as curing

\* Corresponding author.

E-mail address: [yun.gao@ugent.be](mailto:yun.gao@ugent.be) (Y. Gao).

age and water binder ( $w/b$ ) ratio, might be different from pure Portland cement system [22]. However, to the authors' literature study, the relevant research focusing on the microscopic features of ITZ and bulk paste in blended cementitious system is somewhat insufficient, especially about the quantitative aspect. In the previous work, based on experimental and modeling skills, the authors proposed a sound framework for the characterization of ITZ in ternary blended cementitious system [23]. Hereby, some further parallel results are presented on the microscopic features of ITZ and bulk paste, i.e., the effects of hydration factors including replacement levels of SCMs, curing age and  $w/b$  ratio.

A brief introduction on the organization of this paper is given as follows. Section 2 presents some information about raw materials and specimens casting. In Section 3, the relevant research methodologies are introduced, i.e., the experimental measurement via the backscattered electron (BSE) image analysis and the numerical simulation based on the HYMOSTRUC model. In Section 4, the effects of various factors, including SCMs, curing age and  $w/b$  ratio are discussed in detail. Thereafter, some conclusions drawn from this study are presented.

## 2. Materials and specimens

### 2.1. Materials

The current ternary blended cementitious system consists of ordinary Portland cement (cement), blast furnace slag (slag) and limestone filler (filler). Chemical compositions and physical properties of these cementitious materials can be found in Table 1. The laser diffraction test was carried out to measure the relevant particle size distributions, and results are shown in Fig. 1. The sand aggregate has a grain size ranging from 0.1 mm to 1.4 mm with an average density of 2567 kg/m<sup>3</sup>.

### 2.2. Specimens

Three series of mortar specimens are designed with regard to varying replacement levels of SCMs, curing age and  $w/b$  ratio. Details about mix proportions of the designed mortars can be found in Tables 2–4. In particular, mortars listed in Table 2 are used to consider effects of the replacement levels of SCMs, while mortars listed in Tables 3 and 4 are used to investigate the effects of curing age and  $w/b$  ratio. It can be noted that mortars A2, B2 and C2 are actually the same. The use of different symbols is for the sake of comparison. In addition, the aggregate volume fraction for all the mortars is fixed at 10%. As known, for real concrete, a wide range of additional factors in specimen casting, such as bleeding, segregation and compaction are present [24–26]. It is believed that at the 10% vol. aggregate content, if any, effects of these casting factors can be reduced [23].

After sufficient mixing of solids with water, mortars were cast in cubic molds ( $10 \times 10 \times 10$  cm<sup>3</sup>). Then, specimens were vibrated on a vibration table for 2 min. The vibration force was imposed in gravitational direction. Such treatment was expected to reduce the anisotropic effect of further sawn surfaces deliberately. It should be noted that in real concrete, the ITZ often displays anisotropic properties. The fresh mortars were stored in a curing room (95 ± 10% relative humidity and 20 ± 1 °C temperature). After 24 h, specimens were demolded and cured in above-mentioned curing room until the designed age.

**Table 1**  
Chemical composition and physical properties of cementitious materials.

| Chemical composition and physical properties    | Cement | Slag  | Filler |
|---|--------|-------|--------|
| Calcium oxide (CaO, %)                          | 63.37  | 41.83 | –      |
| Silica (SiO <sub>2</sub> , %)                   | 18.90  | 36.32 | 0.80   |
| Alumina (Al <sub>2</sub> O <sub>3</sub> , %)    | 5.74   | 10.72 | 0.17   |
| Iron oxide (Fe <sub>2</sub> O <sub>3</sub> , %) | 4.31   | 0.21  | 0.10   |
| Magnesium oxide (MgO, %)                        | 0.89   | 8.97  | 0.50   |
| Potassium oxide (K <sub>2</sub> O, %)           | 0.73   | 0.37  | –      |
| Sodium oxide (Na <sub>2</sub> O, %)             | 0.47   | 0.27  | –      |
| Sulfur trioxide (SO <sub>3</sub> , %)           | 3.34   | 0.94  | –      |
| Calcium carbonate (CaCO <sub>3</sub> , %)       | –      | –     | 98.0   |
| Insoluble residue (IS, %)                       | 0.41   | 0.25  | –      |
| Loss on ignition (LOI, %)                       | 1.51   | 0.76  | –      |
| Blaine fineness (m <sup>2</sup> /kg)            | 353    | 469   | 753    |
| Specific density (kg/m <sup>3</sup> )           | 3120   | 2896  | 2650   |

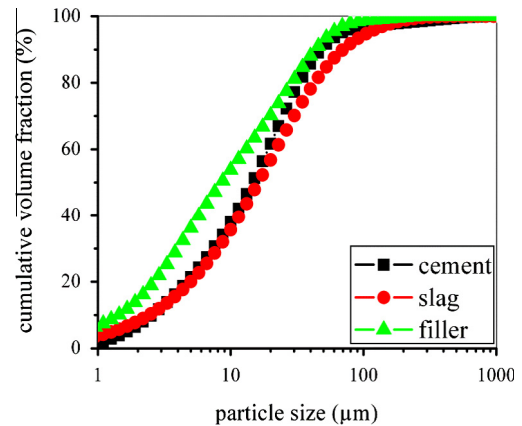


**Fig. 1.** Particle size distributions of cementitious materials, after Ref. [23].

**Table 2**  
Mix proportions for the mortar series A with varying SCMs content.

| Mortar series A | Mass fraction of cementitious material in solid binder (%) |      |        | Curing age (days) | $w/b$ Ratio |
|-----------------|--|------|--------|-------------------|-------------|
|                 | Cement   | Slag | Filler |                   |             |
| A1              | 60   | 0    | 40     | 56                | 0.4         |
| A2              | 60   | 20   | 20     |                   |             |
| A3              | 60   | 40   | 0      |                   |             |
| A4              | 40   | 60   | 0      |                   |             |
| A5              | 30   | 60   | 10     |                   |             |
| A6              | 20   | 60   | 20     |                   |             |

**Table 3**  
Mix proportions for the mortar series B with varying curing age.

| Mortar series B | Mass fraction of cementitious material in solid binder (%) |      |        | Curing age (days) | $w/b$ Ratio |
|-----------------|--|------|--------|-------------------|-------------|
|                 | Cement   | Slag | Filler |                   |             |
| B1              | 60   | 20   | 20     | 28                | 0.4         |
| B2              |  |      |        | 56                |             |
| B3              |  |      |        | 90                |             |

**Table 4**  
Mix proportions for the mortar series C with varying  $w/b$  ratio.

| Mortar series C | Mass fraction of cementitious material in solid binder (%) |      |        | Curing age (days) | $w/b$ Ratio |
|-----------------|--|------|--------|-------------------|-------------|
|                 | Cement   | Slag | Filler |                   |             |
| C1              | 60   | 20   | 20     | 56                | 0.3         |
| C2              |  |      |        |                   | 0.4         |
| C3              |  |      |        |                   | 0.5         |

## 3. Methodologies

### 3.1. Experimental measurement

The backscattered electron (BSE) imaging technique is applied to investigate the microscopic structures of designed mortars [27–29]. In order to acquire qualified BSE images, the following procedures were employed. First of all, specimens were drilled at

Download English Version:

<https://daneshyari.com/en/article/6725559>

Download Persian Version:

<https://daneshyari.com/article/6725559>

[Daneshyari.com](https://daneshyari.com)